IOPscience iopscience.iop.org

Home Search Collections Journals About Contact us My IOPscience

Defects in electron irradiated boron-doped diamonds investigated by positron annihilation and optical absorption

This article has been downloaded from IOPscience. Please scroll down to see the full text article.

2008 J. Phys.: Condens. Matter 20 235225

(http://iopscience.iop.org/0953-8984/20/23/235225)

View the table of contents for this issue, or go to the journal homepage for more

Download details:
IP Address: 129.252.86.83
The article was downloaded on 29/05/2010 at 12:32

Please note that terms and conditions apply.

J. Phys.: Condens. Matter **20** (2008) 235225 (9pp) doi:10.1088/0953-8984/20/23/235225

Defects in electron irradiated boron-doped diamonds investigated by positron annihilation and optical absorption

S Dannefaer[1] **and K Iakoubovskii**[2]

[1] Department of Physics, University of Winnipeg, 515 Portage Avenue, Winnipeg, R3B 2E9, Canada
[2] NIMS, High-voltage Electron Microscopy Station 3-13, Sakura, Tsukuba 305-0003, Japan

Received 26 February 2008, in final form 25 March 2008
Published 9 May 2008
Online at stacks.iop.org/JPhysCM/20/235225

Abstract
Synthetic boron-doped single-crystal diamonds were irradiated by a pulsed electron beam at 2.2 MeV to various accumulated fluences from 0.7×10^{18} to 10×10^{18} $e^- cm^{-2}$. The samples were then subjected to isochronal annealing up to 1260 °C and characterized by positron annihilation (PA) and optical absorption (OA) spectroscopies after each annealing step. PA combined with *in situ* monochromatic illumination gave an estimate for the positive/neutral energy level in the band gap for the monovacancy as ∼0.6 eV above the valence band-edge. From the analysis of PA and OA results, a dominant OA line at 0.552 eV was associated with a neutral boron–interstitial complex, and the annealing temperature of the positive monovacancy was deduced as ∼700 °C.

(Some figures in this article are in colour only in the electronic version)

1. Introduction

Radiation-produced point defects in single-crystalline diamond have been investigated extensively in nitrogen-rich and nitrogen-free samples (type I and IIa, respectively [1–3]). Boron-doped semiconducting diamond (type IIb), on the other hand, has not been investigated nearly as much, especially for high concentrations of acceptors well into the parts per million range. In particular, it is of interest to compare the occurrence of, for example, zero-phonon absorption lines (ZPLs) in type IIa and in type IIb diamond, and also how the strength of ZPLs varies with fluence. Again, in contrast with type I or IIa diamond, the annealing of radiation-produced defects in type IIb diamond appears not to have been investigated much. Note that boron is the most important dopant of synthetic diamond, and the radiation phenomena are intrinsic to all plasma-assisted diamond growth techniques. Therefore, the interaction of boron with radiation-produced defects appears important both scientifically and technologically.

This work concentrates on irradiated type IIb diamond, but because of the fortuitous sample characteristics it was possible to investigate, albeit only optically, defect creation in a part of the sample that was (essentially) type IIa. One aim was to determine the position of the $+/0$ electronic level in the band gap for the monovacancy by means of positron annihilation similar to the case of the $0/-$ level [4]. Another aim was to investigate the physical origin of a prominent ZPL at 0.552 eV in the heavily boron-doped part of the samples, a task made possible by combining optical and positron data.

2. Experimental details

Two high-pressure high-temperature single-crystalline boron-doped diamonds were investigated. They were in the shape of polished 4×5 mm^2 plates with a thickness of 0.6 mm. The samples were dark blue, except for a nearly colourless ∼0.3 mm wide layer along the rim. This layer could be investigated by optical absorption, but was too narrow for positron measurements. In the following, the part along the rim will be referred to as the L-part (L for light), and the rest as the D-part (D for dark). Boron concentration in the D-part was estimated from optical absorption as 5 ppm [5].

Electron radiation was performed with a 2.2 MeV pulsed beam (pulse duration 3 ms, and 240 pulses s^{-1}) with a time-averaged flux of 8×10^{16} $e^- cm^{-2} h^{-1}$; the flux was 40% larger within each pulse. Accumulated fluences at $(0.7, 1.7, 2.7, 3.7, 4.4, 7.4,$ and $10.4) \times 10^{18}$ $e^- cm^{-2}$ were

 © 2008 IOP Publishing Ltd Printed in the UK

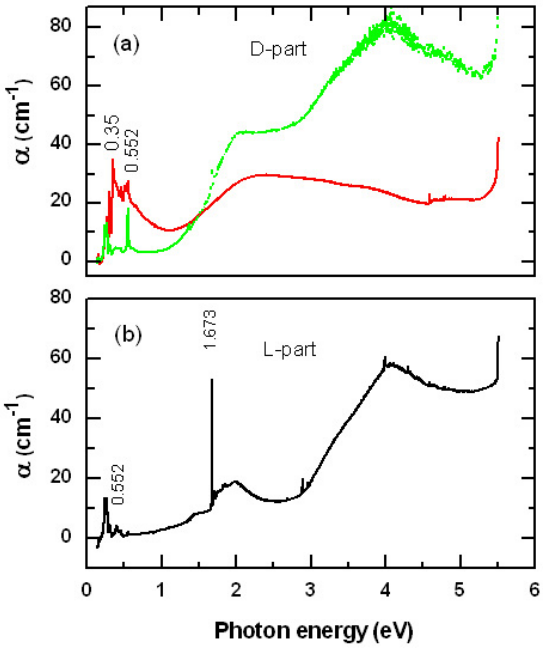

Figure 1. Overview of absorption spectra (77 K) for the electron irradiated boron-rich part D in panel (a) and the boron-lean part L in panel (b). Two spectra are shown in panel (a): one for the fluence of 7.4×10^{18} e$^-$ cm^{-2} (red solid line closer to the bottom at high energies) and the other for 10.4×10^{18} e$^-$ cm^{-2} (green dotted line). The fluence was 4.4×10^{18} e$^-$ cm^{-2} in the case of the L-part.

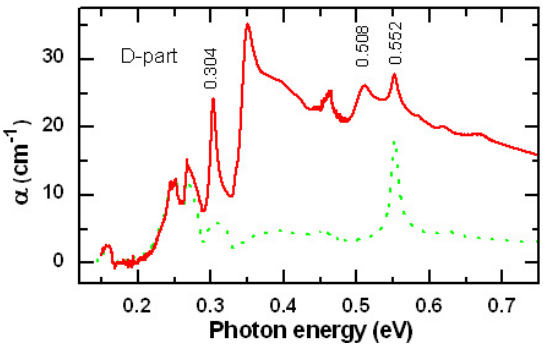

Figure 2. Detail of the absorption spectra (77 K) in the D-part for the two fluences 7.4×10^{18} (red solid line) and 10.4×10^{18} e$^-$ cm^{-2} (green dotted line).

administered to the samples with the samples cooled by rapidly circulating water at 8 °C.

Optical absorption was measured using commercial spectrometers with samples either at 77 or at 293 K. In some cases it was possible to cover the energy range between 0.2 and 5.5 eV, but in the annealing experiments the range between 0.6 and 1.2 eV was not accessible. The spectral resolution was ∼0.2 meV at <1 eV and 1 meV at higher energies.

A general introduction to positron annihilation can be found in [6], whereas [7] contains a review that addresses points of particular interest in the present context. The positron source was a 0.5 mm diameter deposit of 18 μCi ^{22}NaCl on 0.8 μm thick Al foil, and the faint outline of the source on the foil made it possible to place the source reliably between the samples so only the D-part was measured.

Positron lifetime spectra were obtained using a spectrometer with a 190 ps response to prompt gamma quanta at full width at half maximum. Each spectrum contained 1×10^7 counts, and was repeatedly measured six to nine times to reduce the statistical uncertainty of the numerical analysis [8]. In the case of the unirradiated samples, a source correction was applied consisting of a 250 ps, 1.5% component, mimicking the contribution to the lifetime spectra from the source assembly itself. For the irradiated samples, an additional correction was used, as described in section 3.2, in order to extract the data pertinent to radiation-produced vacancies. The analyses also included a 1.5–2.0 ns component with an intensity of 0.05–0.15%.

Doppler broadening of the annihilation quanta was measured using a Ge detector with an energy resolution of 1.2 keV, and each spectrum contained 2×10^6 counts within the annihilation peak at 511 keV: as for lifetime spectra, at least six repetitive measurements were made. The spectra were characterized by the *S*-parameter, which is defined as the ratio between the counts in the energy region of (511 ± 0.7) keV centred at the annihilation peak and that in the (511 ± 4.5) keV region. No source correction is necessary for these measurements, since only relative changes of the Doppler parameter *S* are relevant.

Annealing was performed up to 1260 °C using an ambient of flowing high-purity N_2.

3. Results

This section is divided into three parts, where the first concentrates on optical absorption, the second on positron annihilation, and the third on annealing.

3.1. Optical absorption

Figure 1 shows an overview of absorption spectra for the D- and L-parts of one of the samples for different fluences. In the D-part (panel (a)) the well-known absorption from excitation of holes trapped by the boron acceptor is present at ∼0.35 eV at the lower fluence, but there is also a very small signal from neutral monovacancies (V^o) at 1.673 eV. At the highest fluence an absorption at 0.552 eV, not reported in the most comprehensive data collection [9], increased significantly, whereas absorption at 0.35 eV disappeared and absorption at 1.673 eV increased. In the L-part (figure 1(b)), absorption at 1.673 eV is much stronger and many weaker lines are also apparent, whereas absorptions at 0.35 and 0.552 eV are much weaker than in the D-part.

Figure 2 shows a detail of the spectrum for the D-part for the same two fluences as in figure 1(a). The peak at 0.552 eV shifts upward by 0.004 eV between 77 and 293 K, which is contrary to most optical lines [9]. The peak at 0.508 eV arises from the 1-phonon replica of boron absorption [10], and is weak at the highest fluence.

Table 1 contains a listing of ZPLs in the L- and D-parts, and the integrated absorption for each of the ZPLs is for the fluence of 7.4×10^{18} e$^-$ cm^{-2}. The main line in

Table 1. The positions, labels and areas of zero-phonon optical absorption lines observed in the D-part (boron-rich) and L-part (boron-lean) of a synthetic IIb diamond irradiated by the fluence 7.4×10^{18} e^- cm^{-2}. See figure 3 for an illustration of the fluence dependences of the 0.552 and 1.673 eV ZPLs in the two parts.

ZPL (eV)	Label	Peak area (meV cm^{-1}) L-part	Peak area (meV cm^{-1}) D-part	ZPL (eV)	Label	Peak area (meV cm^{-1}) L-part	Peak area (meV cm^{-1}) D-part
4.584	5RL	8	22	1.861	R2	3	0
3.990	R11	20	0	1.673	GR1	100	0
2.888	GR3	20	0	1.364		1.5	0
2.881	GR2	10	0	0.993		1.0	0.3
2.683		3	0	0.977		0.5	0.1
2.673	TR13	0.5	0	0.904		0.8	0.6
2.638	TR12	2	0	0.793		3.0	0.5
2.463	3H	2	0	0.552		15.0	120

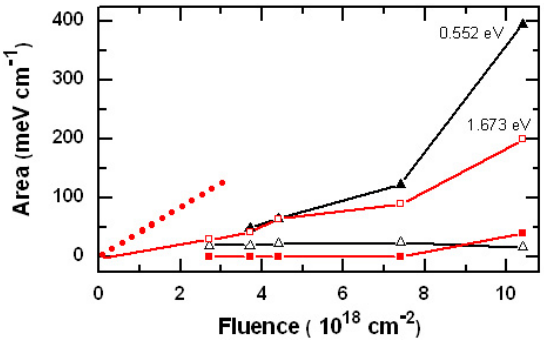

Figure 3. Fluence dependences of 0.552 and 1.673 eV ZPLs. Filled symbols are for the D-part and corresponding open symbols for the L-part. The heavy dotted line segment indicates data from electron irradiated synthetic type IIa diamond of the 1.673 eV ZPL [3, 11]. Lines are only guides to the eye.

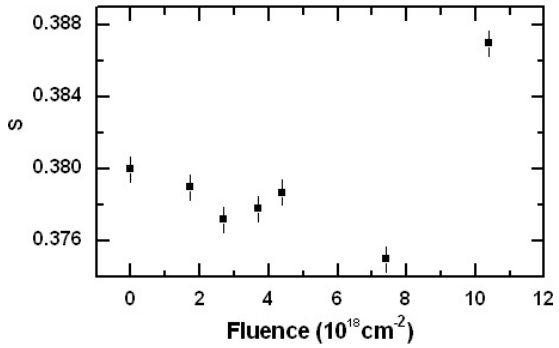

Figure 4. Dependence of the S parameter from the D-part on accumulated fluence measured at room temperature.

the L-part is due to V^o (1.673 eV), while the main line in the D-part is at 0.552 eV, and figure 3 shows their fluence dependences. The slope of the heavy dotted line represents the fluence dependency of V^o absorption from 2 MeV electron irradiation of synthetic IIa diamond [3, 11]. In the L-part, which is essentially type IIa, the slope is initially about three times smaller, but between 7.4 and 10.4×10^{18} cm^{-2} the slopes are nearly equal. In the D-part, V^o is first observed at 7.4×10^{18} cm^{-2}, and the slope corresponds to that in the L-part in the range of the lower fluences.

3.2. Positron data

Table 2 lists positron lifetime and Doppler data for the as-grown D-part of the samples and data for two synthetic type IIa diamonds, since positron measurements were not possible in the L-part. The data in table 2 were obtained at room temperature, but no changes outside experimental error were observed down to 8 K. There is little difference, if any, between the positron parameters for the two types of diamond, and both have a low-intensity lifetime component denoted τ_2 in table 2. It may arise from the positron source itself and/or from grown-in vacancies in the samples but, since the subject matter is the influence from radiation, the τ_2 contribution was removed (technically as a source contribution) in the analyses of the lifetime spectra for the radiated samples.

Table 2. Positron lifetimes, τ_1 and τ_2, and Doppler parameter, S, for as-grown samples (D-part), and for a separate set of type IIa samples, all measured at 293 K. I_2 is the intensity of the τ_2 lifetime component and the intensity of the τ_1 component is $(100 - I_2)$.

Sample type	τ_1 (ps)	τ_2 (ps)	I_2 (%)	S (± 0.0008)
IIb	99.0 ± 0.5	355 ± 8	2.2 ± 0.08	0.3800
IIa	99.1 ± 0.5	350 ± 3	2.6 ± 0.06	0.3792

For accumulated fluences to 7.4×10^{18} cm^{-2}, radiation-produced vacancies could not be detected either at room temperature or at 8 K by means of positron lifetime measurements, but the Doppler technique could detect changes, and they are shown in figure 4. There is a small decrease in S with increasing fluence, accentuated at 8 K, which contrasts the increase in S that usually occurs upon irradiation of IIa diamond. At the highest accumulated fluence (10.4×10^{18} cm^{-2}), S increases distinctly, and vacancies were confirmed by the emergence of the 145 ± 3 ps lifetime due to V^o [7], as well as by GR1 absorption.

Figure 5 shows how the relative change in S, $\Delta S/S_{\mathrm{Ref}}$, varies with measurement temperature after various temperatures of annealing, to be detailed in the following section. S_{Ref} is the S parameter obtained before radiation, and is very close to the bulk S parameter in appendix A. A common feature is that $\Delta S/S_{\mathrm{Ref}}$ is nearly constant up to ~200 K, and then increases with temperature. In the case of electron irradi-

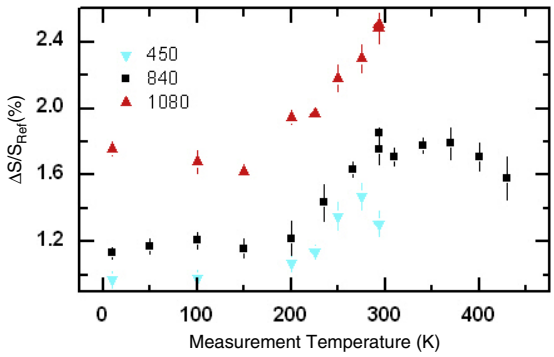

Figure 5. Relative Doppler parameter as a function of sample temperature. $\Delta S/S_{\mathrm{Ref}}$ is $(S - S_{\mathrm{Ref}})/S_{\mathrm{Ref}}$. Data are shown for the samples irradiated to the fluence of 10.4×10^{18} e$^-$ cm^{-2}, and annealed to the indicated temperatures in °C.

ated type IIa diamond the relative increase in S due to V°, i.e. $\Delta S_{\mathrm{V}}/S_{\mathrm{Ref}}$, was found to be $(8 \pm 1)\%$ [7]. In the present case the increase is $(17 \pm 2)\%$, as calculated using the same trapping model as for type IIa diamond (see appendix A), and the reason for the significant numerical discrepancy will be discussed in section 4.1.

Positron lifetime experiments were also performed on the 7.4×10^{18} and the 10.4×10^{18} cm^{-2} radiated samples during illumination by monochromatic light between 0.32 and 3.0 eV. Different responses to the light were found, as shown in figure 6: at the lower fluence, photon energies between 0.6 and 0.7 eV caused a 145 ± 3 ps lifetime to appear, i.e. the same lifetime as detected without illumination, but at the higher fluence. At the highest fluence the positron signals were rather light insensitive.

3.3. Annealing

Isochronal annealing of the 10.4×10^{18} e$^-$ cm^{-2} radiated samples was performed up to 1260 °C, and for each temperature step optical absorption and positron lifetime spectra were measured. Doppler data were also obtained between 8 and 425 K for selected annealing temperatures (cf figure 5). In figure 7 the integrated absorption of the 0.552 eV ZPL is shown in panel (a), and that for the absorption of V° (1.673 eV) in panel (b) as a function of annealing temperature. The width of the 0.552 ZPL decreased from 170 meV below 400 °C to 120 meV above 800 °C. As shown in figure 7(c), annealing above 550 °C creates ZPLs at 2.542 eV (TH5), at 2.445 eV (M2), and at 2.440 (M1) [9], of which TH5 has been identified as arising from divacancies [12].

Absorption due to boron was removed by radiation and remained so up to an annealing temperature of 1080 °C. At 1120 °C it returns, and has at 1260 °C grown to the same value as after the fluence of 4.4×10^{18} cm^{-2} (see figure 7(a)): holes were partially returned to the boron acceptors.

Positron results obtained from the same samples as used for the optical measurements are shown in figure 8. The radiation-produced lifetime is nearly constant up to 600 °C, and then increases steadily with increasing annealing temperature. This is commonly observed, such as in Si [13], and is a consequence of vacancy agglomeration above a certain temperature. The intensity, however, exhibits changes with annealing temperature that contrast common behaviour where the intensity decreases with increasing lifetime due to vacancy agglomeration. Here, the intensity increases and decreases without any significant change in lifetime up to about 600 °C, and the subsequent increase in lifetime above 800 °C has very little effect on the intensity.

4. Discussion

The discussion is divided into four parts, where the first deals with positron data and how boron influences trapping, the second with the optically detected defects, the third with illumination, and the fourth with annealing where positron and optical absorption data are combined. The interpretation of

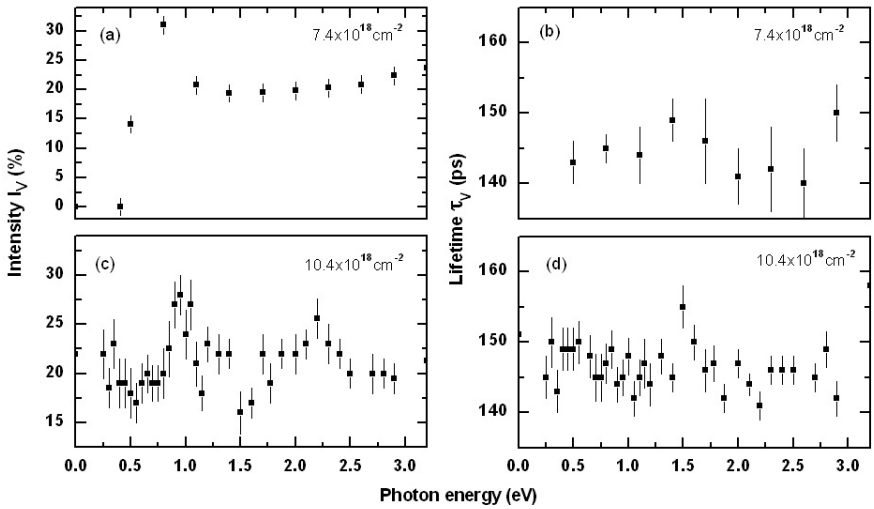

Figure 6. Positron lifetime results (293 K) for samples continuously illuminated by monochromatic light. Data shown in panels (a) and (b) are for the samples irradiated to the fluence of 7.4×10^{18} cm^{-2}, and in (c) and (d) for 10.4×10^{18} e$^-$ cm^{-2}. Note that the 145 ps lifetime component in panel (b) required illumination larger than 0.6 eV to be observable.

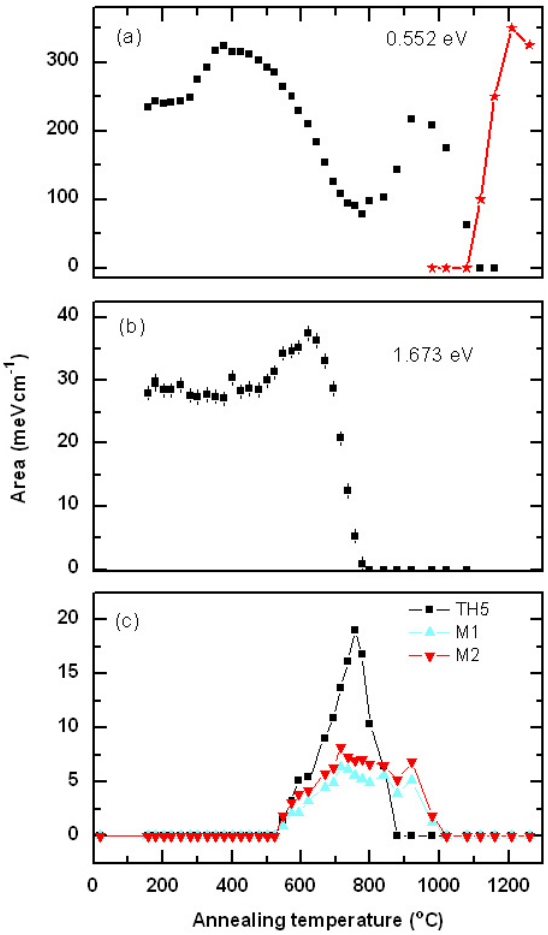

Figure 7. Optical data for isochronal annealing ($\frac{1}{2}$ h) of the D-part after a fluence of 10.4×10^{18} e$^-$ cm^{-2}. In panel (a), the integrated absorption at room temperature of the 0.552 eV ZPL is shown together with the boron absorption at 0.304 eV (stars). Panels (b) and (c) show, respectively, the 1.673 absorption of V^o at 77 K, and those for TH5 (2.542 eV), M1 (2.440 eV) and M2 (2.445 eV).

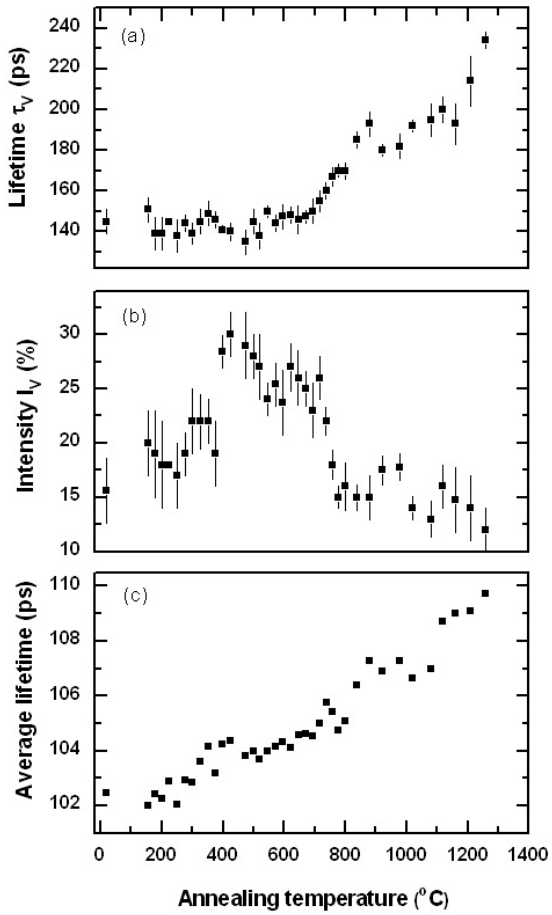

Figure 8. Positron lifetime data (293 K) for the same isochronally annealed samples as used for the optical measurements shown in figure 7. Panel (c) shows the average lifetime, defined as $\tau_1(1 - I_V) + \tau_V I_V$.

the positron data has as its *modus operandi* that *ionized* (or compensated) boron impurities (B$^-$) and vacancies compete in the trapping of positrons.

4.1. Positron data

There are several observations that suggest positron trapping by compensated boron. The strongest case is the value for the monovacancy-specific S parameter. It was 8% larger relative to the bulk value ($\Delta S_V/S_B = 8\%$) in type IIa, but was found to be 17% in type IIb samples after the fluence of 10.4×10^{18} e$^-$ cm^{-2} (see appendix A for details). This contradictory result is explained as a consequence of the omission of competitive trapping from a defect that possesses no vacancy character. As shown in appendix A, this leads to an overestimate of $\Delta S_V/S_B$, but agreement is obtained for a competitive trapping rate of 12 ns^{-1}.

The competitive trap is negatively charged [14, 15] because the S-parameter is significantly lower at ∼100 K than at 300 K (figure 5) and, as will be shown from the annealing experiments, this negatively charged non-vacancy defect remains up to ∼1100 °C. There would appear to be two candidates for the defect, B$^-$ or negatively charged interstitials, but the interstitial option is not viable because in type IIa diamond, with the higher chemical potential (or 'Fermi level'), they would have had the same effect as in IIb diamond, so values for $\Delta S_V/S_B$ should have been the same. We proceed assuming that B$^-$ is the competitive trap.

There are two corollaries from B$^-$ being a trap. The first is that for the two fluences of 7.4×10^{18} and 10.4×10^{18} e$^-$ cm^{-2}, the trapping rate in IIb diamond increases much more slowly than in type IIa diamond [16]. The difference is a factor of five to six, of which most (about five) is ascribable to the reduced response to V^o arising from trapping by B$^-$, thus obtaining a reasonable agreement in the V^o production rate in similar types of diamond. The second is that the unexpected annealing behaviour of the intensity of the lifetime component due to V^o in figure 8 can be explained (in section 4.4) mainly as a consequence of the concentration of B$^-$ varying with annealing.

4.2. Optically detected defects

Within the rim (L-part) the boron concentration is much smaller (by a factor of ∼20) than in the rest (D-part) of the

sample. Numerous ZPLs were found in the L-part (cf table 1), all known from irradiated type IIa diamond with the exception of the 0.552 eV ZPL (according to [9]). Some lines needed a threshold fluence before they could be observed, which indicates that the chemical potential in the L-part was lower in the band gap than commonly encountered in type IIa diamond samples. In the D-part the much higher boron concentration would place the chemical potential even lower (close to 0.4 eV above the valence band [17]), requiring much higher fluences to be observed, as in the case of V^o. The implication is that most, if not all, of the defects observed in type IIa diamond have optically inactive lesser-charged states which are populated when the chemical potential is close to 0.4 eV above the valence band-edge.

The dependence of the integrated absorption on fluence of the dominant ZPLs at 0.552 and 1.673 eV is shown in figure 3, and the data suggest that the former line arises either from a defect only observable when the potential is low, as in the D-part, or from a radiation-produced defect that involves boron as a part of its structure. Since the defect is observed (weakly) and essentially independent on fluence in the L-part, but dependent on fluence in the D-part, this suggests that the defect contains boron. This interpretation of the 0.552 eV ZPL will be substantiated in the discussion of the annealing data, leading to the conclusion that the defect is a neutral boron–interstitial complex.

Several of the ZPLs in the L-part showed a strong increase between the fluences of 7.4 and 10.4×10^{18} e^- cm^{-2}, of which the case of V^o is particularly interesting. The slope of the 1.673 eV absorption in the L-part (cf figure 3) above the fluence of 7.4×10^{18} cm^{-2} is close to that observed earlier in electron irradiated type IIa synthetic diamond, but below that fluence the slope is three times less in the L-part. The same low slope is found in the D-part when V^o becomes observable in that part. The difference between the slopes may arise from differences in the recombination rate between vacancies and interstitials caused by the position of the chemical potential. In the D-part the potential is initially close to the boron acceptor level (0.37 eV), and when V^o appears in the D-part it has increased to ∼0.6 eV according to illumination experiments (see next section). In the L-part the position of the chemical potential relative to the valence band-edge is not well defined because of band bending in the wide depletion layer in the L-part, but is lower than in type IIa diamond. Although the present experiments do not reveal the nature of the processes that are responsible, they do indicate that when the chemical potential is 'well' below mid-gap, the radiation hardness of diamond is increased by a factor of three.

4.3. Illumination: positron data

The effects of illumination on the positron intensity, I_V, for the monovacancy differ significantly for the two fluences investigated (cf figure 6). For the smaller fluence the abrupt increase in I_V for photon energies above 0.6 eV provides strong evidence for electrons being photo-excited and trapped by V^+, thus becoming observable by positrons as V^o. The source for the electrons is most likely the valence band, rather than a defect that can deliver electrons via the conduction band, since the latter possibility would place a donor level 0.6 eV below the conduction band, which is very unlikely for the diamonds studied here. Hence the $+/0$ charge level for the monovacancy is close to 0.6 eV above the valence band-edge, and the $0/-$ energy level was previously found to be 2.5 eV above the valence band-edge [4]. Note that transitions between the $+/0$ or $0/-$ level and the valence or conduction band are not observed in conventional optical absorption spectra. This is probably because of the overlap with the stronger absorption from boron and the 1.673 eV vibronic system.

For the higher fluence the abrupt increase in I_V is missing. This can be explained as a result of V^o and V^+ coexisting, so that a photo-excited electron trapped by V^+ causes the resulting hole in the valence band to be trapped by V^o, and no measurable net effect results.

4.4. Annealing: positron and optical data

The interpretation of the positron annealing data employs as the key point that trapping by vacancies competes with trapping by ionized boron acceptors. The following sections discuss annealing in various temperature ranges and link a ZPL at 0.552 eV with positron data to indicate that the ZPL arises from overall neutral boron–interstitial pairs.

4.4.1. 20–400 °C. The increase in absorption at 0.552 eV (figure 7(a)) coincides with the increase in the intensity of positrons trapped by V^o (figure 8(b)) but, since there is no change in V^o concentration according to optical measurements (figure 7(b)), this means that the competitive trapping by ionized boron is reduced. The reduction is ascribed to positively charged interstitials migrating to ionized boron (not observed by optical absorption), consequently associating the 0.552 eV absorption with a B^-I^+ complex; it is not a positron trap, since it has no vacancy character and it is neutral. The argument could be made that migration of V^+ to B^- can also explain the data, since trapping of positrons by V^+, despite its positive charge, becomes possible due to the proximity of B^-. However, that would mean a fairly low temperature of migration relative to that for V^o (∼700 °C) [2], whereas the interstitial model indicates ∼350 °C for I^+, as for I^o in type IIa diamond [18]. The interpretation implies that the mobility of I^+ is enhanced during radiation, since B^-I^+ complexes are present after radiation, as is also observed for I^o in type IIa diamond [18].

4.4.2. 400–650 °C. The general decrease in I_V in this temperature range is interpreted to be a consequence of a decrease in B^-I^+ concentration, which increases trapping by B^- and hence decreases I_V. However, the increase in V^o concentration between 500 and 650 °C as per optical absorption will, by itself, increase I_V, so two opposing effects are occurring, with the net effect being a decrease.

Annealing of V^o in type IIb and IIa diamond differ in two aspects: in IIb there is no decrease in concentration close to 400 °C as in type IIa diamond, while the increase in V^o concentration between 500 and 650 °C in type IIb is

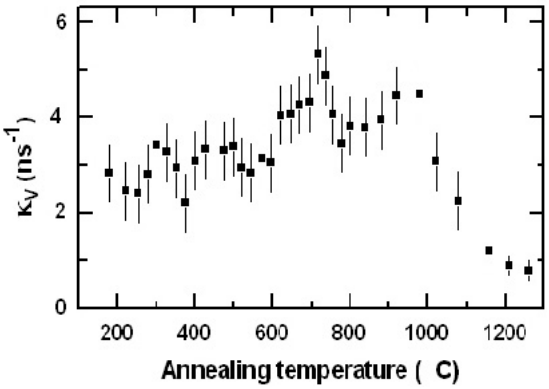

Figure 9. Trapping rate due to vacancies calculated with the assumption that an ionized B impurity is a positron trap at room temperature.

absent in IIa samples [11]. These differences are ascribed to boron, which traps interstitials, hence preventing the annealing of vacancies close to 400 °C, and at the higher temperatures causes charge transfer to generate more V^o from V^+.

4.4.3. 650–1250 °C. Vacancy agglomeration occurs between 650 and 850 °C since the positron lifetime increases from 145 ps to a plateau of 185 ps, and a similar result for IIa diamond [19] was interpreted to arise from the creation of divacancies, V_2. These results correlate reasonably well with the TH5 optical absorption line, interpreted to arise from V_2 with the help of electron paramagnetic resonance [12, 20]. Figure 7 reveals the unusually high (∼0.5) ratio of maximal concentrations of TH5 and 1.673 eV (V^o) peaks; this ratio is about ten times smaller in IIa diamond [12] with the same observation for the M1 and M2 peaks. Considering the large irradiation fluence, it is not the TH5, M1, or M2 intensities that are too high, but rather the V^o concentration that is too small in IIb diamond, because most vacancies are positively charged. Therefore, the strong increase in TH5 upon annealing at ∼700 °C suggests that both V^o and V^+ anneal out around this temperature similar to the case of V^o and V^- [2]. In this respect, diamond differs from other semiconductors, such as Si or SiC, where differently charged vacancies start migrating at rather dissimilar temperatures.

Comparison of optical and positron results from the same sample revealed that TH5 absorption has disappeared at 850 °C (figure 7(d)), but the lifetime remains at 185 ps up to 900 °C. M1 and M2 absorption lines do persist to ∼1000 °C, and we suggest that one or both of them are also associated with V_2. The same conclusion was made in the case of type IIa diamonds [19].

During the increase in lifetime its intensity decreases, but this decrease is not solely a result of divacancy formation, because in type IIa diamond vacancy agglomeration to V_2 gives rise to only a modest decrease [19]. Instead, the decrease in intensity is mainly due to the continuing decrease in B^-I^+ concentration (hence increasing trapping by B^-) until the local minimum at 800 °C is reached. A 'transient' increase in B^-I^+ concentration peaks at 1000 °C and that, too, is reflected by the increase in I_V, albeit modified because further vacancy agglomeration is evident, which by itself would decrease the intensity.

It is noteworthy that at 1120 °C, and above, the absorption at 0.35 eV returns, showing that deeper trapping sites for holes than B^- are disappearing. After annealing at 1260 °C it is estimated that about 70% of the holes are returned to the boron acceptors, as based on the increase in the 1-phonon replica line at 0.508 eV. The remaining 30% of the holes are still trapped somewhere, and the traps may well be vacancy or interstitials clusters.

4.4.4. Vacancy concentration. The qualitative arguments for the model presented in the preceding sections, and detailed in appendix A, can be used to calculate the positron trapping rate for vacancies (cf appendix B), which is of physical importance since it is proportional to the vacancy concentration. A trapping rate of 1 ns^{-1} corresponds to a concentration of 2 ppm neutral monovacancies [14, 15], a calibration that is accurate to within 30%. The model yields the positron trapping rate from ionized boron acceptors in terms of the concentration of B^-I^+ complexes (equation (B.2)), and with equation (A.9) the vacancy trapping rate is obtained. Figure 9 shows that the trapping rate varies, but not significantly, up to 1080 °C, the highest temperature to which the model applies. There is a ∼40% increase in trapping rate between 500 and 650 °C, and nearly the same increase (30%) was observed for the absorption due to V^o (cf figure 7(b)). Above 650 °C vacancy agglomeration occurs, causing a modest decrease in trapping rate, exactly as found earlier in the case of vacancy agglomeration in type IIa diamond [19].

It was mentioned above that absorption from boron acceptors returns at temperatures above 1120 °C. Since absorption from B^-I^+ has disappeared, we may assume that the difference between the original uncompensated boron absorption and the present one arises from ionized boron, and we can use the same model as before to calculate κ_V at the three highest temperatures. The continuous decrease in trapping rate from vacancies above ∼1000 °C is due to gradual vacancy agglomeration. Electron paramagnetic resonance has indicated vacancy agglomeration beyond the size of V_2 at temperatures above 800 °C, with the tentative assignment of V_3 and V_4 agglomerates as the main species [21], and the modest increase in positron lifetime to ∼220 ps supports that interpretation. The average size of these vacancy clusters is significantly smaller than is encountered in natural brown diamonds (where the lifetime is ∼435 ps [22, 23]) and might correspond to four to six monovacancies.

The influence of ionized boron on the trapping of positrons by vacancies was ascribed qualitatively to the temperature dependence of $\Delta S/S_{\mathrm{Ref}}$ shown in figure 5. Using the data in table 3, and assuming that the only temperature-dependent parameter is the trapping rate arising from B^- (a very reasonable assumption), it decreases by a factor of three going from 200 to 293 K for each of the annealing temperatures in figure 5. This temperature dependence substantiates that a negatively charged defect with no vacancy character is trapping positrons.

Table 3. Summary of lifetime and Doppler results (at 293 K) for different annealing temperatures of the 10.4×10^{18} e^- cm^{-2} radiated samples. κ_V is the trapping rate for vacancies and κ_1 is that for ionized boron acceptors. The last column contains data for the monovacancy obtained on type IIa diamond [7], where κ_1 is zero due to the absence of boron.

Annealing temperature (°C)	Lifetime (ps)	κ_V (ns^{-1})	κ_1 (ns^{-1})	$\Delta S/S_{Ref}$ (%)	$\Delta S_V/S_{Ref}$ (%)	$\Delta S_V/S_{Ref}$ (IIa) (%)
293	142 ± 3	3.8 ± 0.2	12 ± 2	1.2	8	8.0 ± 1
450	142	3.8	6.5	1.4	8	
840	180	4.9	22	1.8	13	
1080	195	3.2	15	2.4	19	

5. Conclusions

Based on results obtained using two experimental techniques (OA and PA) applied to the same samples, the following conclusions can be drawn.

An absorption line at 0.552 eV at 77 K (0.556 eV at 293 K) is suggested to arise from an overall neutral boron–interstitial complex formed during radiation and, additionally, by thermal annealing close to 400 °C: there is no well-defined annealing temperature for the defect, but it persists up to ∼1100 °C.

Based on positron data, the +/0 electronic level for the monovacancy is located 0.6 eV above the valence band-edge, placing it well below that for the 0/− level at ∼2.5 eV.

The rate at which radiation damage is introduced by 2.2 MeV electrons depends on the position of the chemical potential within the band gap, being smaller by a factor of about three when the potential is less than ∼0.7 eV from the valence band-edge. Annealing of neutral and positively charged vacancies occurs close to ∼700 °C.

Vacancy agglomeration takes place in two stages, the first starting at ∼600 °C, where divacancies are formed giving rise to TH5, M1, and M2 absorption lines, and the other above ∼1000 °C, where larger clusters are gradually formed. Above 1120 °C, some of the radiation-produced hole-traps anneal out and absorption due to uncompensated boron reappears.

Acknowledgments

This work was made possible by the financial assistance of the Natural Science and Engineering Research Council of Canada (NSERC), and by de Beers, who supplied the samples. Dr Carl Ross, National Research Council, Ottawa, Canada, is especially acknowledged for the electron irradiation.

Appendix A

We consider a variation on the conventional trapping model [6] in which positrons in addition to vacancy traps, giving rise to an annihilation rate λ_V, can also be captured by a trap with negligible vacancy character, i.e. having an annihilation rate equal to that for the bulk (in this context, the trap is the ionized boron acceptor). De-trapping at room temperature is assumed not to take place, so the lifetime spectrum will then have the form

$$\dot{S}(t) = (\lambda_B + \kappa_1 + \kappa_2)(1 - I_2 - I_3)\exp(-(\lambda_B + \kappa_1 + \kappa_2)t) + \lambda_B I_2 \exp(-\lambda_B t) + \lambda_V I_3 \exp(-\lambda_V t), \quad (A.1)$$

where κ_1 and κ_2 are the trapping rates for positrons trapped by boron acceptors or by vacancies, respectively. The bulk annihilation rate is λ_B (equal to 10 ns^{-1} [7, 24]) and the I s are the intensities of the lifetime components. They are given by

$$I_2 = \frac{\kappa_1}{\lambda_B - \lambda_V + \kappa_1 + \kappa_2}, \quad (A.2)$$

and

$$I_3 = \frac{\kappa_2}{\lambda_B - \lambda_V + \kappa_1 + \kappa_2}. \quad (A.3)$$

Suppose that the first two components in equation (A.1) cannot be resolved so that analyses of experimental spectra must be done with two components,

$$\dot{S}_{exp}(t) = \lambda_1(1 - I_3)\exp(-\lambda_1 t) + \lambda_V I_3 \exp(-\lambda_V t). \quad (A.4)$$

In equation (A.4) the reasonable assumption was made that the last term arising from vacancies survives intact, but the two shorter lifetimes are 'lumped' into a single annihilation rate λ_1.

In the least-square analysis used to determine λ s and I s, it is most probable that the pre-exponential terms in the first two components in equation (A.1) equal that for the first component in equation (A.4), i.e.

$$\lambda_1(1 - I_3) = (1 - I_2 - I_3)(\lambda_B + \kappa_1 + \kappa_2) + I_2\lambda_B \quad (A.5)$$

and, using equations (A.2), and (A.3), we find that

$$\lambda_1 = \lambda_B + \kappa_2 - \frac{I_3}{1 - I_3}\kappa_1. \quad (A.6)$$

The trapping rate from the approximate analysis is

$$\kappa_2' = \frac{I_3}{1 - I_3}(\lambda_B - \lambda_V). \quad (A.7)$$

However, the real trapping rate for vacancies comes from equation (A.3) and is

$$\kappa_2 = \frac{I_3}{1 - I_3}(\lambda_B - \lambda_V + \kappa_1), \quad (A.8)$$

or

$$\kappa_2 = \kappa_2' + \frac{I_3}{1 - I_3}\kappa_1. \quad (A.9)$$

In the absence of the λ_B component in equation (A.1), κ_2' equals κ_2, so the proper value for κ_2 is, of course, deduced from the analysis, but otherwise the trapping rate for vacancies is underestimated.

For Doppler data, assuming that the S parameter for positrons trapped at the ionized boron acceptor equals S_B, the experimentally determined S parameter can be written as,

$$S = \left(1 - \frac{\kappa_2}{\kappa_1 + \kappa_2 + \lambda_B}\right) S_B + \frac{\kappa_2}{\kappa_1 + \kappa_2 + \lambda_B} S_V \quad \text{(A.10)}$$

where subscripts in S_B and S_V stand for bulk and vacancy, respectively. Defining S_V–S_B as ΔS_V and $S - S_B$ as ΔS (experimentally determined), it follows that $\Delta S_V/S_B = \Delta S/(FS_B)$, where $F = \kappa_2/(\kappa_1 + \kappa_2 + \lambda_B)$. Similarly, for the approximate analysis $\Delta S'_V/S_B = \Delta S/(F'S_B)$, where $F' = \kappa'_2/(\kappa'_2 + \lambda_B)$. Using $I_3 = 20\%$ according to figure 8 as an average value below 400 °C, $\Delta S'_V/S_B$ is 17%, but should have been 8%, as mentioned in section 4.1. From the definitions of F and F' and equation (A.9), we find that $\kappa_1 = 12$ ns^{-1} and $\kappa_2 = 3.8$ ns^{-1} will produce the 8%.

Appendix B

Let the concentration of uncompensated boron before irradiation be $[B_o]$. After a fluence of 10.4×10^{18} cm^{-2}, all boron acceptors are compensated, so

$$[B^-]_{irr} + [B^-I^+]_{irr} = [B_o], \quad \text{(B.1)}$$

allowing for the possibility that some of the ionized boron acceptors (B^-) are complexed with interstitials during irradiation. B^-I^+ is the boron–interstitial complex that is claimed to give rise to the 0.552 eV absorption. As mentioned earlier (section 4.1), the trapping rate κ_1 of $[B^-]_{irr}$ is 12 ns^{-1}, and that for vacancies, κ_2, is 3.8 ns^{-1}. After annealing at 450 °C, κ'_2 is 1.2 ns^{-1} according to equation (A.7) and, since κ_2 did not change because the concentration of V^o is constant, κ_1 from $[B^-]_{irr}$ is 6.5 ns^{-1}, as calculated from equation (A.9). The decrease in κ_1 corresponds to an increase in the integrated absorption from 240 to 324 meV cm^{-1} according to figure 7(a), giving the calibration

$$\kappa_1 = -0.065A + 27.6 \text{ (ns}^{-1}\text{)}. \quad \text{(B.2)}$$

A is the integrated absorption at 0.552 eV at room temperature in units of meV cm^{-1}. With equation (A.9), the trapping rates from vacancies are shown in figure 9.

References

[1] Davies G 1977 *Chemistry of Carbon* 13 (New York: Dekker) pp 1–143
[2] Davies G, Lawson S C, Collins A T, Mainwood A and Sharp S J 1992 *Phys. Rev.* B **46** 13157
[3] Kiflawi I, Collins A T, Iakoubovskii K and Fisher D 2007 *J. Phys.: Condens. Matter* **19** 046216
[4] Pu A, Avalos V and Dannefaer S 2001 *Diamond Relat. Mater.* **10** 585
[5] Burns R C, Cvetkovic V, Dodge C N, Evans D J F, Rooney M-L T, Spear P M and Welbourn C M 1990 *J. Cryst. Growth* **104** 257
[6] Krause-Rehberg R and Leipner H S 1999 *Positron Annihilation in Semiconductors* (Berlin: Springer)
[7] Pu A, Bretagnon T, Kerr D and Dannefaer S 2000 *Diamond Relat. Mater.* **9** 1450
[8] Kirkegaard P, Pedersen N J and Eldrup M 1989 *PATFIT-88 Risø Report M-2740* Risø, DK-4000 Roskilde, Denmark
[9] Zaitsev A M 1998 *Handbook of Industrial Diamonds and Diamond Films* (New York: Dekker)
[10] Smith S D and Taylor W 1962 *Proc. Phys. Soc.* **79** 1142
[11] Iakoubovskii K, Kiflawi I, Johnston K, Collins A T, Davies G and Stesmans A 2003 *Physica* B **340–342** 67
[12] Lea-Wilson M A, Lomer J N and van Wyk J A 1995 *Phil. Mag.* B **72** 81
[13] Dannefaer S, Avalos V, Kerr D, Poirier R, Shmarovoz V and Zhang S H 2006 *Phys. Rev.* B **73** 115202
[14] Mascher P, Dannefaer S and Kerr D 1989 *Phys. Rev.* B **40** 11764
[15] Puska M J and Nieminen R M 1994 *Rev. Mod. Phys.* **66** 841
[16] Dannefaer S, Mascher P and Kerr D 1992 *Diamond Relat. Mater.* **1** 407
[17] Collins A T 2000 *J. Phys.: Condens. Matter* **14** 3743
[18] Hunt D C, Twitchen D J, Newton M E, Baker J M, Anthony T R, Banholzer W F and Vagarali S S 2000 *Phys. Rev.* B **61** 3863
[19] Dannefaer S, Pu A, Avalos V and Kerr D 2001 *Physica* B **308–310** 569
[20] Twitchen D J, Newton M E, Baker J M, Anthony T R and Banholzer W F 1999 *Phys. Rev.* B **59** 12900
[21] Iakoubovskii K and Stesmans A 2004 *Phys. Status Solidi* a **201** 2509
[22] Avalos V and Dannefaer S 2003 *Physica* B **340–342** 76
[23] Hounsome L S, Jones R, Martineau P M, Shaw M J, Briddon P R, Öberg S, Blumenau A T and Fujita N 2005 *Phys. Status Solidi* a **202** 2182
[24] Uedono A, Fujii S, Morishita N, Itoh H, Tanigawa S and Shikata S 1999 *J. Phys.: Condens. Matter* **11** 4109